Numerical modeling of open-ended piles

Nasser Sekfali[1*], *Brahim* Lafifi[2]

[1] Badji Mokhtar-Annaba University, Department of Architecture, Annaba, Algeria, nasser.sekfali@univ-annaba.dz
[2] 8 Mai 1945-Guelma University, Civil Engineering and Hydraulics Department

Abstract. Deep foundations are generally used when significant loads are applied, and the site conditions do not allow for the implementation of soil reinforcement processes. This research focuses on studying the behavior of piles in a frictional environment, used as foundations for offshore structures in dense sands, involving anchor depths and overloads significantly higher than those encountered in onshore applications. The bearing capacity of open-ended driven piles plays a crucial role in this study. Therefore, a series of tests were conducted in the literature on model piles in a calibration chamber, which is considered a tool for physical modeling, allowing for significant penetration of instrumented model piles under confinement conditions similar to those experienced by real piles. Emphasis is placed on predicting the ultimate load capacity of open-ended piles using numerical methods. Calculations were performed using the finite element code PLAXIS to numerically reproduce the same shear stresses as those measured on the model during various phases of the experiment. The approach aims to validate the documented experiments in the literature and compare the ultimate load capacity of an open-ended pile to that of a closed-ended pile. Our study is limited to the case of a single pile, subject to static and axial force. The results show that it is possible to achieve a good agreement between the experiment and the numerical modeling with a relatively simple model, provided that the soil parameters are chosen correctly and the interface stiffness is adequately simulated.

1. Introduction

These are piles specifically designed for use in marine environments, and they have particular characteristics. They are open-ended tubular metal piles, with lengths reaching up to 100 meters and diameters exceeding 1.5 meters. They are systematically installed by driving. Soil is pushed inside the tube until it reaches sufficient resistance to prevent any further penetration, thus creating a 'plug'. The penetration of the pile is halted if the internal friction, increased by the weight of the plug, exceeds the bearing capacity of the soil beneath the pile tip. Significant theoretical and experimental research has been conducted at the former Institut Mécanique in Grenoble, now known as the 3SR Laboratory, on the issue of deep foundations, with a focus on open-ended piles. The design principles of these piles, based on field tests, chamber tests, and systematic methods, have been studied by various researchers [1-4]. These principles are widely applied in offshore foundation design. The work of Dessaint [5], as well as the research by Biarez and Gressillon [6], Foray and Puech [7], has contributed to linking the tip resistance to the compressibility of granular materials under high stresses.

The impact of various installation methods on the values of tip resistance and lateral friction has been studied by Genevois [8] and Mokrani [9] through physical modeling in a calibration chamber in Grenoble. Kyuho et al [10], from load tests on open-ended and closed-ended piles driven into sand, observed that the unit ultimate resistance at the base of open-ended piles was 31% and 51% lower than the corresponding values for closed-ended piles. Experiments on model piles in clayey soil showed that the ultimate load of open-ended piles was 91% compared to that of closed-ended piles [11]. Calibration chamber tests conducted by Lech Balachowski [12] confirmed a slower mobilization of tip resistance for open-ended piles, with an open-ended pile reaching only about 80% of the resistance of the closed-ended pile for a displacement equal to one-tenth of the diameter.

In this study, a numerical modeling of Lech Balachowski's experiments [12] was conducted using the finite element software PLAXIS, aiming to replicate the calibration chamber tests. Simulation results showed a maximum deviation of (4%) between experimental and numerical results, demonstrating good agreement between the two methods. Comparisons of tip resistances revealed that open-ended piles reach approximately 77.16% of the resistance of closed-ended piles, supporting the findings of Lech Balachowski [12].

2. Experimental Test Results

For the continuous driving tests conducted in the calibration chamber, the tip resistance obtained for open-ended model piles in dense sand was examined based on different failure criteria, with w/d ratios ranging from 0.1 to 1. Table (1) summarizes the results of the tests performed on open-ended piles, presenting the failure criteria (0.3 and 1).

Table 1. Calibration chamber test results [12]

Test 92-2 Dense sand, Smooth pile $\sigma'_v = 400\ Kpa$			
w/d	τ mean KPa	head force KN	q_p MPa
0,3	160 (130)	78 (81)	13,1 (14,3)
Test 92-4 Dense sand, Rough pile $\sigma'_v = 400\ Kpa$			

* Corresponding author: nasser.sekfali@univ-annaba.dz

w/d	τ mean KPa	head force KN	q_p MPa
0,3	210 (240)	79 (91)	11,9 (12,2)
Test 93-1 Dense sand, Rough pile $\sigma'_v = 500\ Kpa$			
w/d	τ mean KPa	head force KN	q_p MPa
1	-	- (132)	- (12,8)

Note: Values in parentheses correspond to the second cycle of static loading.

3. Finite Element Modeling

Calibration chamber experiments were conducted by LECH BALACHOWSKY [12] with the aim of examining the bearing capacity of an open-ended pile driven by driving into dense sand, and comparing it to the results obtained by MOKRANI [9] and GENEVOIS [8] for a closed-ended pile. Due to the overconsolidation of sands in the North Sea, they also addressed the issue of modeling open-ended piles in overconsolidated sand. To replicate in the laboratory the stress conditions along offshore piles, which often exceed forty meters in length, they applied effective vertical stresses to the chamber, ranging between 400 and 600 kPa.

The objective of our study is to develop a numerical model (reference model) to replicate numerically the cast-in-place pile tests using PLAXIS 8.2 software. Subsequently, we aim to establish a comparison of the bearing capacity between an open-ended pile and a closed-ended pile. For an accurate simulation of these experiments, we have modeled the stresses induced along the piles during the mass conditioning and their evolution during static loading.

4. Materials used

4.1 The test pile

This is a pile provided by IFP and consists of a steel tube with a thickness of 4 mm and an outer diameter of 70 mm.

The pile has been cut to a length of 1650 mm. Originally, its surface was smooth. However, to achieve roughness according to the specified standard, sand grains of the same material used for the tests were adhered to its surface. The outer diameter of the rough pile is now 76 mm, as illustrated in Figure (1). The pile is embedded in the tank at a depth of 80 cm, and then a static load is applied with a prescribed displacement. This load is applied using a mechanical jack with a capacity of 150 kN, equipped with a gear motor and a controller allowing speed adjustment in a range from 0 to 20 mm/minute.

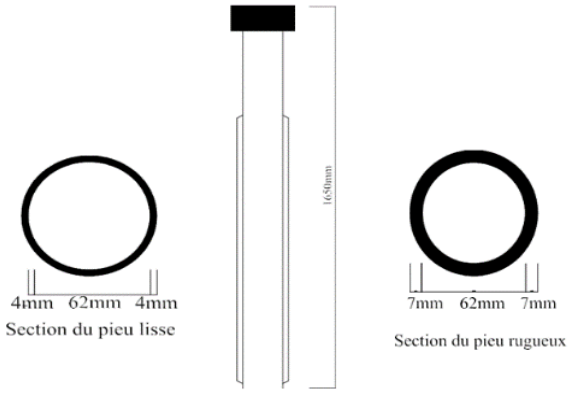

Fig. 1. The model pile used for calibration chamber tests

4.2 The sand

This is a quartz sand extracted from the Hostun quarry in Drôme. This material is characterized by angular grains and a uniform grain size distribution. We report the mechanical properties of this sand in Table (2), which have been extracted from experimental curves based on the work of MOKRANI [9].

Table 2. Values of E_P, E_t, and E_{tmax}according to the vertical surcharge [9]

$\sigma'_v(Kpa)$	$E_p(Mpa)$	$P_c(Kpa)$	$\varphi(°)$	$\sigma_m(Kpa)$	$E_t(Mpa)$	$E_{tmax}(Mpa)$
100	26	161,4	45,8	96	26	223
200	37	127,2	43,2	117	36	269
400	256	517,0	41,9	340	76	415
500	418	583,0	41,7	400	96	452

5. Reference Model

5.1 Geometry of the model

The model is geometrically represented by lines and points. It is defined by 14 points representing the tank of the calibration chamber, which has dimensions of 1.50m in height and 1.20m in diameter. The problem is axisymmetric, and only π radians of the pile will be modeled with a distribution of triangular elements with 15 nodes and interface elements represented in Figure (2).

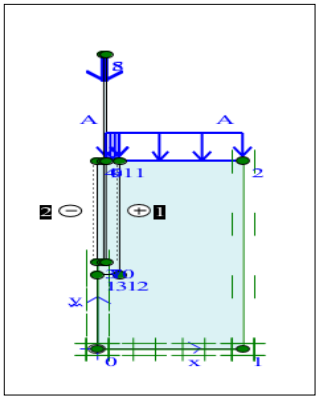

Fig. 2. Geometry of the problem (smooth pile Test 92-2).

5.2 The behavior models used

5.2.1 The elastic model

This model is generally used to simulate structural elements made of concrete or metal in interaction with the soil. It is employed to model the steel pile with an annular section, using a Poisson's ratio of $\nu_p = 0{,}2$ and a Young's modulus E = 210 GPa.

5.2.2 The Mohr-Coulomb model

This model allows describing the behavior of soil in an elastic-perfectly plastic manner, both under monotonic and cyclic loading. It requires the determination of five parameters: the Young's modulus E, the Poisson's ratio ν, the cohesion C, the friction angle φ, and the dilation angle ψ. Table (3) compiles the physico-mechanical parameters of the two materials.

Table 3. The parameters of the Elastic and Elasto-plastic Mohr-Coulomb models [9].

Parameters	Name	Dense Hostun sand		steel pile	Units
Material type	Material Model	Mohr-Coulomb		Linear Elastic	-
		smooth pile	Rough pile		
behavior type	Material type	Drained	Drained	Non-pourous	-
Saturated unit weight	γ_{sat}	18,7	18,7	-	[KN/M^3]
Dry unit weight	γ_{unsat}	16,7	16,7	71,5	[KN/M^3]
Horizontal permeability	K_x	-	-	-	[M/Jour]
Vertical permeability	K_y	-	-	-	[M/Jour]
Young's modulus	E^{ref}	76000	76000 96000	210000000	[KN/M^2]
Cohesion	C^{ref}	0,2	0,2	-	[KN/M^2]
Poisson's ratio	ν	0,3	0,3	0,2	-
Angle of internal friction	φ	41,9	41,9 41,7	-	[°]
Angle of dilatancy	ψ	11,9	11,9 11,7	-	[°]

The normal stiffness of the interface, defined as a linear function of the shear modulus G, is a crucial parameter for determining the mobilization of friction. Garnica [13] used a highly sophisticated soil behavior law, assuming a constant shear modulus along the entire length of the pile. Mokrani [9], on the other hand, adopted a linear increase in the shear modulus with depth during pressuremeter tests conducted in the calibration chamber of the 3S laboratory. In our study, we also considered a linear increase in the shear modulus with depth. This is the initial tangent modulus for Hostun sand RF, and this linear increase in the G modulus with depth can be simulated in PLAXIS by introducing a low fictitious cohesion into the sand.

5.3 The Mesh

To generate the mesh of the homogeneous soil mass, PLAXIS allows us to automatically mesh the problem, with the possibility of refining it locally. It consists of 306 elements, 2733 nodes, and 3672 constraint points for the various piles. Figure (3) depicts a typical mesh of the problem with axisymmetric conditions.

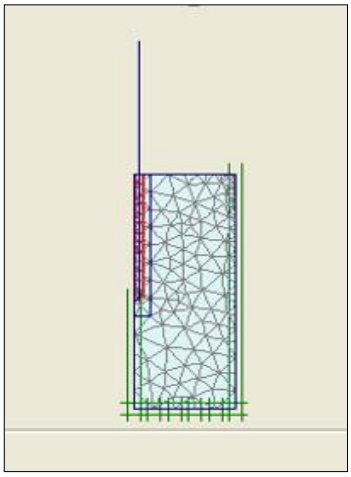

Fig.3. Mesh of the problem (smooth pile Test 92-2).

5.4 The Loading

In our model, we can define two distinct types of loadings. The first type of loading represents the distributed surcharge on the soil mass, thus conditioning the stress state along the pile. The equivalent value of this loading should correspond to that applied during laboratory experiments, divided by π. The second type of loading corresponds to statically applied loading with imposed displacement. It is achieved by introducing values so that the vertical displacement component is directed towards the negative Y direction. The displacement values to be introduced will be applied in multiple phases, following the criteria presented in Table (4).

Table.4. Values of the imposed displacements

Test number	Pile type	Vertical Overload	Imposed Displacements (w/d) en (m)
Test 92-2	Smooth	400 KPa	0,007 0,014 0,021
Test 92-4	Rough (Standard)	400 KPa	0,0076 0,0152 0,0228
Test 93-1	Rough (Standard)	500 KPa	0,0076 0,0152 0,0228 0,038 0,076

5.5 Initial Conditions

Once the geometric model is created and the finite element mesh generated, the initial stress state and the initial configuration must be specified. This is done in the section dealing with initial conditions in the data input program. The initial conditions consist of two different modes, one to generate initial interstitial pressures (hydraulic conditions mode figure 4) and the other to specify the initial geometric configuration and generate the initial effective stress field (geometric configuration mode). In the second mode, PLAXIS proposes a default value for K_0 based on the formula of Jaky.

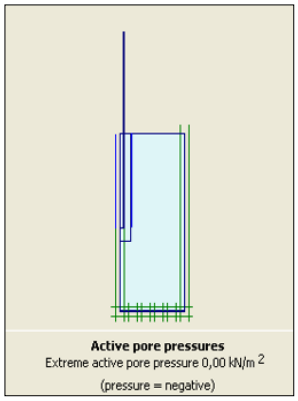

Fig.4. Interstitial pressure (smooth pile Test 92-2)

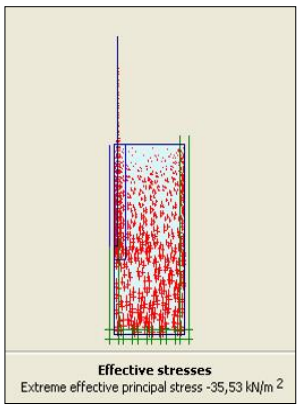

Fig.5. Effective stresses (smooth pile Test 92-2)

5.6 Calculation Type

The calculations will be performed for an axisymmetric analysis and will start as soon as the initial conditions state is generated. These calculations will be carried out in the same manner in the elasto-plastic modeling for the various test piles. Plastic calculation has been chosen, and it is desired that the loading continues automatically until the required ultimate level is reached. This loading is constructed in several stages, meaning that each calculation phase must be resolved iteratively.

6. Results

The primary results of a finite element simulation include displacements and stresses. During the calculation phase, it is crucial to select the locations at which we wish to visualize the results, both for displacements (nodes) and stresses (Gauss points). Additionally, the corresponding ultimate load is obtained and expressed in kN/radian.

6.1 The main results (smooth pile Test 92-2)

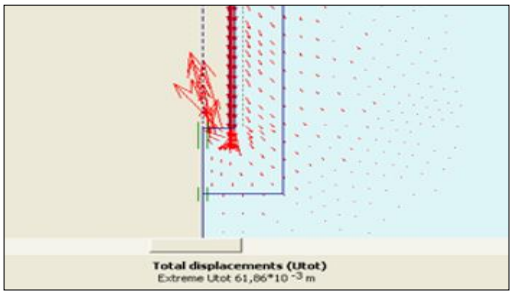

Fig. 6. Incremental displacement field (smooth pile Test 92-2)

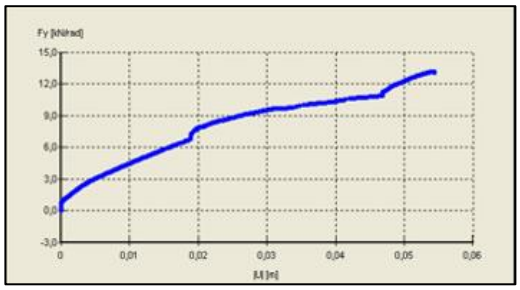

Fig. 7. Load-displacement curve (smooth pile Test 92-2)

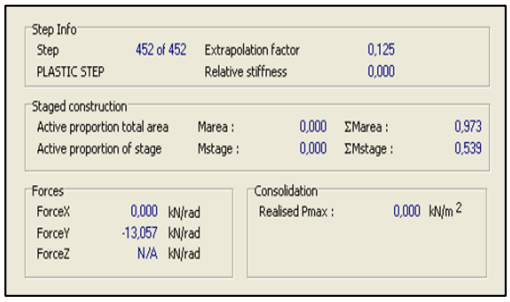

Fig. 8. Calculation summary (smooth pile Test 92-2)

The incremental displacement field is a valuable indicator of the kinematics.

In this section, we can gather information regarding the progress of the calculation (figure, 7). For instance, the total force along the Y-axis amounts to 13.057 kN/radian (figure, 8), which corresponds to an ultimate load on the pile of approximately (13.057 * 2 * 3.14) = 81.99 kN. The results for the other types of piles are summarized in Table (5).

Table 5. Ultimate load values at the final loading stages.

N° Tests	Criterion w/d (m)	q_p (Mpa)	
		Experimental Results	Numerical Results
Test 92-2	0,3	13,1 (14,3)	13,057
Test 92-4	0,3	11,9 (12,2)	11,506
Test 93-1	1,0	- (12,8)	15.741

6.2 Comparison: Open-ended/Closed-ended Pile

We have just compared the tip resistance obtained by driving two piles, one open-ended and the other closed-ended, with the same dimensions (70mm in diameter), the same type of sand, and under the same confinement conditions.

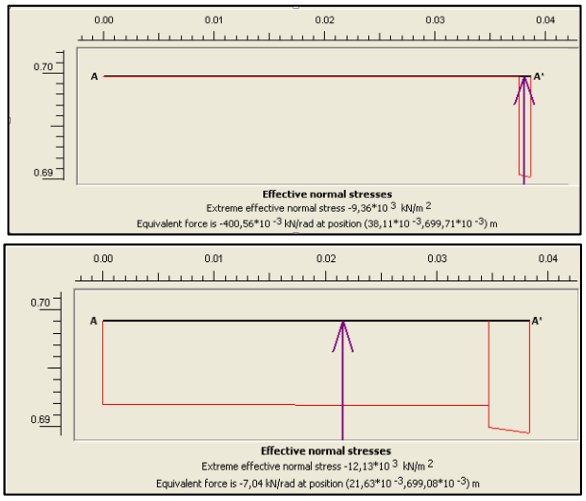

Fig. 9. Effective Normal Stress (Open and Closed Pile)

Figure (9) illustrates the effective normal stress at the base of both the open-ended and closed-ended piles. These results are summarized in Table (6), including the corresponding ultimate tip loads.

Table 6. Ultimate Tip Load of Open and Closed Piles

Pile	Effective Normal Stress σ_n' KN/m²	Ultimate Tip Load Q_p KN
Open-ended	9360,00	36,00
Closed-ended	12130,00	46,66

7 Conclusion

The pile penetration results were similar to those obtained during the tests, especially for the failure criterion (w/d = 0.3), with a maximum deviation of (4%). This confirms that the Mohr-Coulomb model with small strain is considered an appropriate model to represent the behavior of tubular piles and allows for satisfactory convergence between experimental and numerical results using the PLAXIS software. The comparison of tip resistance revealed that open-ended piles reach approximately 77.16% of the resistance of closed-ended piles, confirming BALACHOWSKI's conclusion.

References

1. J. Klos, A. Tejchman, Analysis of Behavior of Tubular Piles in Subsoil, Proceedings of the 9thinternational conference on Soil Mechanics and Foundation Engineering, Tokyo, Vol. **1**, pp. 605-608, (1977).
2. American Petroleum Institute (API), Recommended Practice for Planning, Designing and Constructing of Fixed Offshore Platforms –RP2A-LRFD, 19th Edition, Washington (1991).
3. M. F. Randolph, M. May, E.C. Leong, and G. T. Houlsby, One-Dimensional Analysis of Soil Plug in Pipe Piles, Géotechnique Vol. **41**, No. 4, pp. 587-598, (1991).
4. R. J. Jardine, R. F. Overy, F. C. Chow, Axial Capacity of Offshore Piles in Dense North Sea Sands, Journal of Geotechnical and Geoenvironmental Engineering, ASCE, Vol. 124, No.2, pp.171-178, (1998).
5. A. Dessaint, Contribution à l'étude de la force portante limite des fondations profondes en milieu homogène, Thèse de Doctorat, Université de Grenoble (1966).
6. J. Biarez, J.M. Grésillon, Essai et suggestion pour le calcul de force portante des pieux en milieu pulvérulent, Vol.**22**, N°2, pp.433-450, (1973).
7. P. Foray, A. Puech, Influence de la compressibilité sur la force portante à la rupture des pieux en milieu pulvérulent, Annales de l'institut Technique du Batiment et des Travaux Publics, N° 131, (1976).
8. J.M. Genevois, Capacité portante des pieux à grande profondeur. Simulation physique à l'aide d'une chambre de calibration, Thèse de Doctorat, Université Joseph Fourier-Grenoble I (1989).
9. L. Mokrani, Simulation physique du comportement de pieux à grande profondeur en chambre de calibration, Thèse de doctorat à I.N.P.G., Grenoble (1991).
10. P. Kyuho, S. Rodrigo, L. Junhwan, K. Bumjoo, Behavior of Open- and Closed-Ended Piles Driven into Sands. Geotechnical and Geoenvironmental Engineering 129(4) 296-306 (2003).

11. M.J.M. Al-Waily, M.S. Al-Qaisi, Comparison of plugging impact of open-ended with closed-ended model piles in clayey soils. Arabian Journal of Geosciences 14:1909 1-12 (2021).
12. L. Balachowski, Différrents aspects de la modélisation physique du comportement des pieux en chambre d'Etalonnage et Centrifugeuse, Thèse de Doctorat à I.N.P.G., Grenoble (1995).
13. P. Garnica-Anguas, Simulation numérique du frottement entre solides par équations intégrales aux frontières et modèle d'interface non linéaire. Application aux pieux, Thèse de Doctorat, Université Joseph Fourier-Grenoble I (1993).